Development of an integrated hydrothermal liquefaction and wet oxidation process: a pathway for an autothermal biorefinery

Journal of Cleaner Production 521 (2025) 146242

Contents lists available at ScienceDirect

Journal of Cleaner Production

journal homepage: www.elsevier.com/locate/jclepro

Development of an integrated hydrothermal liquefaction and wet oxidation process: a pathway for an autothermal biorefinery

Guido Ceragioli [a,b], Carolin Eva Schuck [b], Giulia Zoppi [b,*], Giuseppe Pipitone [a], Konstantinos Anastasakis [b], Samir Bensaid [a], Raffaele Pirone [a], Patrick Biller [b]

[a] Department of Applied Science and Technology, Politecnico di Torino, Corso Duca degli Abruzzi 24, 10129, Turin, Italy
[b] Department of Biological and Chemical Engineering, Aarhus University, Hangøvej 2, 8200, Aarhus N, Denmark

HIGHLIGHTS

- Batch HTL of straw and manure yielded 37–45 % carbon to biocrude, highest at 350 °C.
- WO can create heat by oxidizing the HTL-AP, which contains 20–29 % of initial carbon.
- An optimal HTL-WO integrated process configuration was identified.
- Exothermic heat from WO is sufficient to achieve integrated autothermal HTL-WO process.
- Energy return on investment is improved from HTL standalone from ~3 to ~7.

GRAPHICAL ABSTRACT

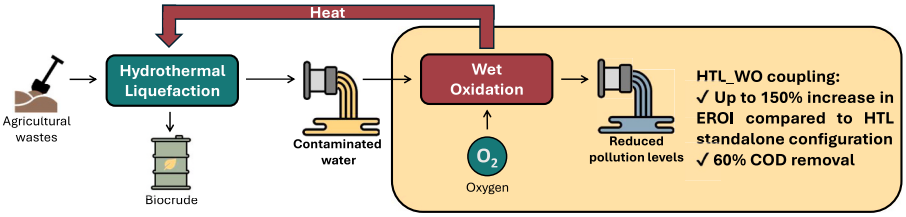

ARTICLE INFO

Keywords:
Hydrothermal liquefaction
Wet oxidation
Process modeling
Wastewater valorization
Biomass conversion

ABSTRACT

Hydrothermal liquefaction (HTL) is set to become a breakthrough technology for producing advanced biofuels, particularly suitable for hard-to-abate sectors. However, HTL faces significant challenges such as high heating demands and aqueous phase (AP) management. This study investigates, from an energy efficiency perspective, the integration of HTL with wet oxidation (WO), an exothermic process which oxidizes organic pollutants in water. The goal is to utilize the heat generated by WO to sustain the high-temperature energy requirement of the HTL process, aiming for autothermal operation. Batch HTL experiments were performed under various temperatures and residence times with wheat straw and cattle manure as feedstocks. The biocrude yield ranged from 24.8 % to 31.4 %, with a HHV between 28.7 and 32 MJ/kg while the AP exhibited a chemical oxygen demand ranging from 45 to 56 g/L. WO was simulated in Aspen Plus® V9 to assess heat generation and AP output composition. The HTL-WO energy integration and standalone HTL processes were then simulated and compared using MATLAB®, which incorporated experimental data, WO simulation results, and an optimized heat exchanger network to assess the corresponding energy expenditures. The integration achieved autothermal operation in several scenarios and demonstrated clear energy efficiency enhancements even when autothermicity was not fully reached, highlighting its robustness. Remarkably, the energy return on investment (EROI) increased by 1.3–3.0 times compared to standalone HTL, reducing the overall energy expenditures from 2.74 to 2.92 MJ/$kg_{dryfeedstock}$ in the HTL standalone process to 0.99–2.29 MJ/$kg_{dryfeedstock}$ in HTL-WO integration.

* Corresponding author.
E-mail address: gzoppi@bce.au.dk (G. Zoppi).

https://doi.org/10.1016/j.jclepro.2025.146242
Received 13 November 2024; Received in revised form 16 May 2025; Accepted 18 July 2025
Available online 28 July 2025

1. Introduction

In the context of global warming, the transportation sector emerges as a major player, ranking as the second-largest contributor to greenhouse gas emissions (ca. 25 % of total globally). Furthermore, it strongly relies on fossil fuels, which make up 90 % of its energy sources (IEA, 2023). Among possible options, the adoption of biofuels holds a significant promise to reduce emissions and provide a renewable alternative to conventional energetic sources, especially for hard-to-abate sectors such as aviation and shipping (IEA, 2021).

In HTL, biomass undergoes treatment at moderate temperatures (250–350 °C), high pressure (5–25 MPa), and high humidity (70–90 % moisture) for variable durations (5–60 min) (Ghadge et al., 2022). Four outputs are generated: the primary product is the so-called biocrude, an apolar phase which presents moderately high heating value (ca. 30 MJ/kg) (Lu et al., 2022); however, due to its high content of heteroatoms (O, N), biocrude requires an upgrading step to be used as liquid biofuel (Ramirez et al., 2015). Moreover, the process produces a solid residue, referred to as hydrochar, which contains 5–35 % of feedstock's carbon and the majority of the feedstock's inorganics; a gaseous stream, mainly composed of CO_2; and an aqueous phase (HTL-AP) with 20–50 % of feedstock's carbon. The distribution of carbon across these different phases is determined mainly by the characteristics of the starting feedstock and the HTL set temperature and residence time (Watson et al., 2020).

Among the array of advanced biofuel conversion technologies, hydrothermal liquefaction (HTL) emerges as a prime candidate due to its minimal pretreatment requirements in terms of energy-intensive drying and its versatility to convert most biomass feedstocks.

The HTL-AP presents one of the major obstacles for the widespread implementation of the technology due to its high chemical oxygen demand (COD). Its treatment or utilization must be addressed to enhance the sustainability of the process from a technical, economic and environmental point of view (Kulikova et al., 2023). Several technologies for HTL-AP utilization have been investigated in literature, such as algae production, anaerobic digestion, bioelectrochemical systems, hydrothermal gasification, recirculation, electrochemical oxidation and aqueous phase reforming (Matayeva and Biller, 2021; Watson et al., 2020; Zoppi et al., 2023). Another option that has recently garnered attention is wet oxidation (WO) (Kilgore et al., 2023; Silva Thomsen et al., 2024; Tews and Garcia-Perez, 2022).

WO is an exothermic hydrothermal treatment in which the degradation of organic compounds is carried out in water under an oxidative atmosphere (e.g., pure oxygen or air). The treatment is suitable for highly organic and toxic wastewaters, with a COD of 10–80 g_{O2}/L (Mishra et al., 2017). The process usually involves temperatures and pressures between 125 and 350 °C and 0.5–20 MPa to maintain the water in the liquid state and to enhance the solubility of oxygen, increasing reaction rates, ionic strength, and production of free radicals (Debellefontaine et al., 1999; Dietrich et al., 1985). The process effectiveness depends on temperature, oxygen concentration, residence time and reactivity of the dissolved molecules. Ideally, a complete oxidation process would convert organic compounds into carbon dioxide, water and ammonia. However, in most cases, only partial oxidation occurs, leading to the formation of intermediate products (such as acetic acid) through a free radical mechanism (Debellefontaine and Foussard, 1999).

The use of WO after HTL has primarily been studied focusing on its effectiveness in reducing water contamination. For example, Silva Thomsen et al. (2024, 2022) achieved up to 98 % and 95 % COD removal through WO in batch and continuous experiments, respectively. Similarly, Prasad Vadlamudi et al. (2024) demonstrated in a laboratory setup that WO of the AP from HTL of manure can achieve 85–90 % removal of TOC and COD. However, the literature does not indicate the potential energetic exploitation of the reaction exothermicity within an integrated HTL-WO configuration.

The goal of WO integration is simultaneously addressing two major energy requirements of the HTL process: thermal demand and wastewater treatment. In fact, despite its advantages, HTL remains an energy-intensive process, where energy allocation and efficiency are not straightforward. These aspects depend on various factors, including feedstock characteristics, operating conditions, product yields and quality, by-product valorization, heat recovery strategies, and system boundaries (Mazhkoo et al., 2025). Recent study highlights that thermal demand is the primary contributor, averaging 35 % of HTL overall energy requirements (Cheng et al., 2020). When considering HTL alone, excluding upstream (feedstock harvesting and transportation) and downstream processes (wastewater treatment and biocrude upgrading), energy consumption ranges from 0.8 to 1.7 MJ/$kg_{dry\text{-}feed}$, with thermal energy accounting for 70–88 % of the total (Hussain and Anastasakis, 2025; Snowden-Swan et al., 2022). Moreover, integrating wastewater treatment into the HTL system can more than double energy duties (Maqbool et al., 2024).

To address this, a batch experimental campaign was first conducted to evaluate HTL at different operative conditions. A mixture of cattle manure and wheat straw was chosen as feedstock, being readily available agricultural residues and according to the promising results reported in previous works (Dos Passos et al., 2022; He et al., 2021; Moser et al., 2023). Subsequently, based on experimental and literature data, WO process was simulated to investigate the influence of reaction conditions (inlet temperature, oxygen flowrate, residence time) on both the released thermal power and effectiveness of HTL-AP COD removal. Finally, HTL and WO were integrated, and the energetic efficiency of the coupled configuration was compared with respect to the standalone option in terms of energy return on investment (EROI). This ensures a common baseline for evaluating the benefits of process integration, allowing for a consistent comparison between the coupled and standalone configurations.

Filling this gap, this study aims to unveil a novel approach that could significantly enhance the energy efficiency of HTL processes, potentially transforming carbon-laden wastewater into a valuable energy resource.

2. Materials and method

This section outlines the experimental procedures and analytical methods employed in this study. It details the HTL experiments, characterization techniques for the obtained products, and the process modeling approach used to evaluate HTL standalone and integrated HTL-WO configurations.

2.1. HTL tests

Wheat straw was harvested at Aarhus University's facilities at Foulum, Denmark. Cattle manure was collected at the Danish Cattle Research Centre (DKC) at Foulum, Denmark. Both wheat straw and cattle manure were dried in oven overnight at 105 °C.

The selection of these feedstocks is based on their synergistic biocrude yield, complementary moisture content, and abundance as agricultural residues in Northern Europe, making them both practical and sustainable feedstocks (Dos Passos et al., 2022; T. Horschig et al., 2020).

Batch HTL reactions were conducted using 26 mL bomb-type reactors, following the procedure detailed in previous studies (Biller et al., 2016; Dos Passos et al., 2022). For each experiment (performed in duplicate), 11 g of slurry, consisting of 15 wt % dry matter mixture of 50 wt % cattle manure and 50 wt % wheat straw, were loaded into the reactor. The reactors were submerged in a preheated FTBLL12 Fluidized Temperature Bath at setpoint temperature and for the desired residence time. The combination of three reaction temperatures (300, 325 and 350 °C) and three reaction times (10, 20 and 30 min) was investigated. The pressure corresponded to the autogenous water vapor pressure at the set temperatures (85.9, 120.5, and 165.3 bar, respectively).

Afterwards the reactor was quenched to room temperature in water. Gas mass determination was performed by weight difference after

venting. The HTL-AP was collected and stored at 4 °C for further analysis. The biocrude and hydrochar were recovered from the reactor using dichloromethane (DCM). The hydrochar and biocrude were separated by vacuum filtration. The solid phase was dried overnight at 105 °C, weighed, and collected for further analysis. DCM with the dissolved biocrude was left to evaporate completely to determine the biocrude mass yield. Gas, biocrude and hydrochar yields were calculated using equation (1), where x refers to the specific phase (gas, biocrude or hydrochar) and m_{feed} refers to the amount of dry biomass fed to the reactor:

$$yield_x = \frac{m_x}{m_{feed}} \quad (1)$$

HTL-AP yield was calculated by difference. All errors were estimated using standard deviation.

2.2. Characterization of the products

The elemental composition (CHNS) of biomass, hydrochar, and biocrude was determined by Elementar vario MACRO cube analyzer (Langenselbold, Germany). The gaseous phase was assumed to be constituted only by carbon dioxide, in compliance with the gas composition of selected samples analyzed with GC-FID-TDC (Agilent Technologies) which confirmed more than 85 % of CO_2, 6 % of CO and less than 2 % of H_2 and alkanes; in accordance with literature findings (He et al., 2021; Madsen et al., 2015; Toor et al., 2012).

Biocrude and hydrochar high heating values (HHVs) were evaluated by Channiwala and Parikh (2002) correlation, Equation (2):

$$HHV\left(\frac{MJ}{kg}\right) = 0.3491C + 1.1783H + 0.1005S - 0.1034O - 0.0151N - 0.0211Ashes \quad (2)$$

Biomass ash content was evaluated following the EN ISO 18122-2015 (ISO: Global standards for trusted goods and services, 2022). Dry biomass elemental composition, ash analysis, and their HHVs are depicted in Table S1.

Chemical oxygen demand (COD) and NH_4 content of HTL-AP were determined through spectrophotometer Spectroquant® Prove 600 using cuvette tests. Five tests were conducted on random samples to measure ammonia content, and the average of these five tests was applied to all HTL-AP conditions.

Total carbon (TC) and total nitrogen (TN) contained in AP samples were evaluated with a scalar FORMACS HT-I TOC/TN analyzer. TC was assumed equal to total organic carbon (TOC) since the inorganic carbon was considered negligible due to the feedstock's nature.

The aqueous phase was further analyzed using a GC-FID 7890A (System 7890A, Agilent Technologies, USA), equipped with an HP-INNOWAX column (30 m, 0.25 μm, 0.25ID, Agilent Technologies, USA) using helium as carrier gas. Hydrogen and air were used for FID detector gases. Some key volatile fatty acids (VFAs), such as acetic acid, propanoic acid, isobutyric acid, pivalic acid, butyric acid, isovaleric acid, valeric acid, isoexanoic acid, hexanoic acid, and heptanoic acid were identified and their composition quantified via external calibration curves.

Carbon and nitrogen balances were evaluated with the procedure reported in paragraph S1 of supplementary material.

2.3. Process modeling

The process modeling is divided into three sections. The first step focuses on finding the optimal process layout considered for the simulations. To achieve this, some simplifications are assumed, and literature data is used to evaluate and identify the heat exchanger configurations.

The second step involves the utilization of a previously developed kinetic WO model in Aspen Plus (Schuck et al., 2023) to obtain more accurate data regarding the heat released during WO of manure-straw HTL-AP.

Finally, a MATLAB code was implemented with the aim to compare the two processes setup from an energetic point of view. The batch experimental HTL data, the WO simulation results, and the optimal heat exchanger were considered simultaneously.

2.3.1. HTL standalone and HTL-WO integration process definition

The process mass flow rate input was set to 1 kg/s of slurry, with 15 % dry matter of 50/50 % straw/manure. HTL reaction conditions were set at 325 °C and 20 min and the corresponding experimental product yields from batch HTL experiments were employed for the mass balance in the model. The HTL pressure was set to 220 bar.

The considered process scheme for the standalone HTL configuration consisted of a single heat exchanger (HEX) (countercurrent, ΔT_{min} = 15 °C) and two trim heaters (TH), as illustrated in Fig. 1. In this configuration, the use external heat is essential to meet the HTL thermal requirements. The use of two trim heaters allows for a reduction in the high-temperature heat input, thereby improving the overall exergy efficiency of the system.

The temperature and pressure for product separation were based on the experimental conditions used in the Aarhus HTL pilot plant (Anastasakis et al., 2018). This entails hot separation of the hydrochar and its humidity was assumed equal to 35 %, with the moisture having the same composition as the HTL-AP. The remaining HTL products are cooled and isolated by gravimetric separation at 70 °C and 3 bar. In this standalone HTL configuration the HTL-AP is assumed to be sent directly to a wastewater treatment (WWT) plant.

A detailed table is provided in supplementary material listing the equivalent temperature, pressure, and mass flow rate for each of the numbered streams (Table S2).

In the HTL-WO integrated configuration, it was essential to determine the WO inlet temperature (T_{inWO}). This temperature is required to achieve a WO outlet temperature of 350 °C, which was set as the maximum attainable temperature to guarantee a safety distance from critical conditions. To this end, two key literature references on WO were considered. The first, by Debellefontaine et al. (1999), reports that the heat released per unit of oxygen reacted is 435 kJ/molO2 reacted. The second, by Silva Thomsen et al. (2022), describes a COD removal rate of 72.6 % for a reaction time of 10 min at 350 °C. The iteration of the combined use of these two data was crucial for the first assessment of T_{inWO}.

The aqueous phase from the product separation stage is pressurized up to 220 bar and needs to be heated up to the WO inlet temperature (T_{inWO}). Subsequently, it is mixed with an oxygen rich gaseous stream composed by 95 % O2 and 5 % N2 (as the typical oxygen-rich concentrations produced in industry (Bai et al., 2021)). The gas is assumed to be compressed by a 3-stage intercooled compressor up to 220 bar, where the third stage is not intercooled to not waste useful heat. The feed enters the WO reactor, where the oxidation reactions generate heat, causing an increase in temperature of the stream. Subsequently, the hot water can be utilized as a heating source within the process prior to the separation of the resulting WO products.

Following these assumptions, it was possible to employ the pinch point analysis with a ΔT_{min} of 15 °C with the purpose of finding an optimal configuration network of four main streams: slurry heating, slurry cooling, aqueous phase heating, aqueous phase cooling. The specific heat capacity (cp) variation of each stream was considered with an accuracy of 5 °C.

2.3.2. WO process simulation

Wet oxidation process was simulated using Aspen Plus® following the work conceptualized by Schuck et al. (2023).

The Aspen process flowsheet used in this paper is shown in Fig. 2. The Peng-Robinson (PENG-ROB) method was used, with exception of

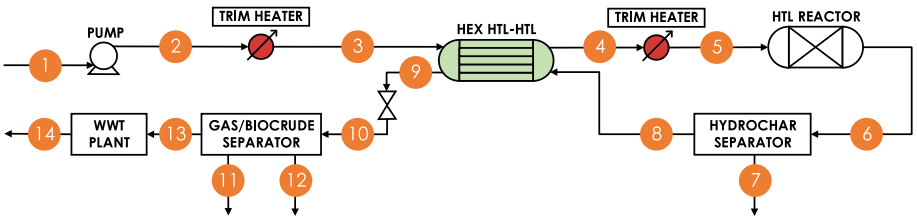

Fig. 1. Process scheme network for HTL standalone configuration. In red the external heat requirement, in green the internal heat recoveries. (For interpretation of the references to colour in this figure legend, the reader is referred to the Web version of this article.)

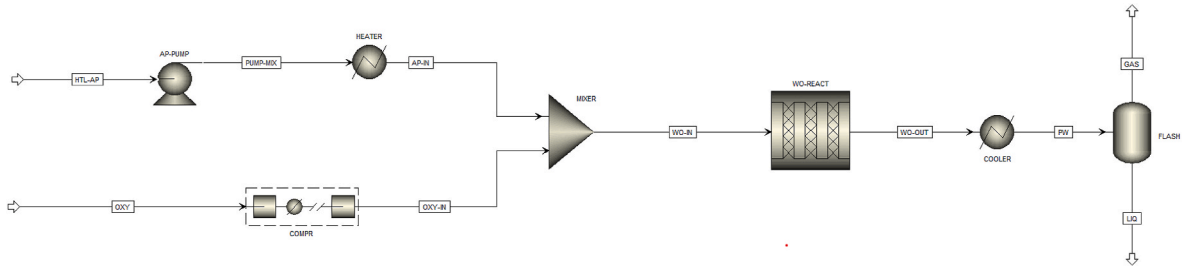

Fig. 2. – WO Aspen plus model layout.

the flash separator for which the Non-random two-liquid (NRTL) activity model was employed to better manage the components subdivision between liquid and vapor phase, introducing Henry components.

According to the work of Schuck et al. (2023) the WO process was rigorously modeled using kinetic data from 13 representative components of HTL-AP. The kinetic data for each component were sourced from literature (Pruden and Le, 1976; Shende and Levee, 1999; Williams et al., 1975) and individually verified according to the original experimental data before being incorporated into an overall RBatch model. Experimental data from batch-scale WO experiments (Silva Thomsen et al., 2022) validated the multi-reaction kinetic model with Aspen RBatch reactor across various temperatures and residence times, enabling its scale-up by integrating an RPlug reactor block (Schuck et al., 2023).

The concentration of each component was evaluated to match the global COD, TOC, TN of the experimental results. The complete procedure is described in paragraph S2 of supplementary material.

The stoichiometric oxygen mass flow rate was calculated with respect to the COD (mg_{O2}/L) of the specific HTL condition.

The initial simulations were conducted to explore the process behavior by varying the oxidant mass flow rate, the reaction time (5–60 min, maintaining the HTL-AP inlet temperature fixed at 300 °C) and the HTL-AP inlet temperature (280–320 °C, with a constant reaction time of 10 min).

Afterwards the inlet temperature after the heater (AP-IN stream in Fig. 2) was set to ensure an outlet temperature of 350 °C from the WO reactor (WO-OUT stream in Fig. 2) for different reactor times (5–60min). The relative length of the reactor was determined to evaluate its practical feasibility.

These initial analyses, focused solely on the HTL case at 325 °C for 20 min as representative of average HTL conditions, allowed identification of the optimal oxygen maximum flow rate (i.e., the rate that maximizes the adiabatic temperature rise in the WO reactor).

The following step involved simulating the WO process for each HTL-AP condition using the optimal oxygen mass flow rate for the chosen length determined earlier. This was done to determine: process inlet temperature, residence time, outlet gaseous and liquid composition after flash separation, and finally COD removal, calculated as follows in Equation (3):

$$COD_{rem}(\%) = \frac{COD_{in} - COD_{out}}{COD_{in}} * 100 \quad (3)$$

All the values of COD outlet streams are obtained by Aspen property "chemical oxygen demand for mixture".

2.3.3. *Energetic analysis*

The two process configurations were simulated and compared using a MATLAB script, which incorporates all data acquired from the HTL experimental batch campaign and the WO Aspen Plus simulations. It evaluates the energy expenditures and heat duties of both trim heaters and heat exchangers. The logic behind the stream couplings is detailed in paragraph S3 of supplementary material, an accuracy of specific heat capacity variation of 5 °C was used.

The energy return on investment (EROI) was used as an indicator to compare the HTL stand alone and the integrated HTL-WO configurations. EROI is defined as the ratio of process power output with respect to the inputs, as reported in Equation (4) and (5). An EROI greater than unity is a prerequisite for a process to be considered sustainable from an energetic viewpoint (Lambert et al., 2014).

The relative EROI equations are reported as follows, where *k* stands for the specific oxygen production technology (as will be shown below).

$$EROI_{HTL-WO} = \frac{\dot{m}_{biocrude} * HHV_{biocrude}}{P_{ox,k} + P_{comp,k} + P_{pump} + P_{th} + P_{WWT}} \quad (4)$$

$$EROI_{HTL} = \frac{\dot{m}_{biocrude} * HHV_{biocrude}}{P_{pump} + P_{th} + P_{WWT}} \quad (5)$$

The primary power expenditures were identified and assessed using empirical relationships integrated into the script. Detailed explanations of these relations can be found in paragraph S4 of supplementary material. P_{pump} represents the power requirements to pressurize the slurry and the aqueous phase (in HTL-WO integration configuration) to 220 bar. Then, power for oxygen production (P_{ox}) and compression (P_{comp}) were evaluated. Three different small/medium scale oxygen technologies with different energy requirements were considered: pressure swing adsorption (PSA), electrolyzers (PEM) and oxygen transport membranes (OTM). It is important to highlight that the latter is not yet available in the market and is taken as a potential future scenario. Specific consumption (SC) (kWh/ $Nm^3_{o_2}$) and the production outlet pressure p_{prod} (bar), which are key parameters for modeling the technology, are

presented in Table 1 with the relative reference used for the estimation.

The compression expenditures for each technology were evaluated starting from their production pressure up to 220 bar.

The HTL reactor heat losses were evaluated considering it as an 8 passes shell and tube reactor. Specific information on reactor heat losses and design are described in paragraph S5 of supplementary material. The heating losses from the reactor are not considered in the definition of autothermal operation.

The trim heaters supply additional heat whenever the system operates under non-autothermal conditions. Total thermal power requirements (P_{th}), represented by trim heaters and HTL heat losses, were supposed to be satisfied using electrical trim heaters with a thermal efficiency equal to 0.95.

Finally, the process wastewater is assumed to be treated to reach the European limit for effluent discharge, equal to 125 mg_{O_2}/L (Council of the European Union, 1991). The cleaning power requirement (P_{WWT}) for a WWT plant was evaluated based on classical aerobic treatment, with a specific power requirement of 0.9 kWh/ $kg_{COD_{removed}}$ (Maqbool et al., 2024; Wan et al., 2016).

For the combined HTL-WO configuration, the combinations of 9 conditions of hydrothermal liquefaction (HTL) and 3 different oxygen production technologies for WO process resulted in a total of 27 distinct scenarios, while for HTL standalone process it reduced to the 9 HTL conditions.

3. Results and discussion

This section presents the results from the HTL batch tests, including product yields and quality. Following this, the optimal HTL-WO integration scheme is introduced, with the corresponding WO Aspen simulation results. Finally, the energy expenditures and the EROI for both the standalone HTL process and the integrated HTL-WO process modeling are reported.

3.1. Hydrothermal liquefaction batch

In Fig. 3 the yield variations for the HTL batch experimental campaign are depicted for different residence times and reaction temperatures.

It can be observed that the biocrude yield varied between a minimum 24.8 % up to 31.4 %; the aqueous phase ranged between 21.4 and 36.2 %; the solid yield was between 15.2 and 24 %, while the gas yield changed between 13.9 and 32.4 %. However, within the investigated range, no significant trend was observed concerning biocrude phase. In contrast, for aqueous phase and hydrochar, a decrease in yield was observed with increasing temperature, which favored the production of gaseous products.

A direct comparison can be made with previous works where the synergistic effect of cow manure and wheat straw was studied under various temperature and concentration conditions (Dos Passos et al., 2022). The results reported in this study align well with those found in the existing literature.

Apart from the biocrude yield, it is also important to evaluate the biocrude composition, which entails the final possibility of using it as fuel. In Table S3 the elemental analysis of biocrude is reported. Also in this case, no clear trend is present in terms of carbon, oxygen, and nitrogen concentration in the biocrude. However, it is worth highlighting that the final HHVs were in the 27.2–32.0 MJ/kg range, with higher values reached at higher temperatures. These results are in line with previous works on HTL from different feedstocks. The CHNS analysis of hydrochar, presented in Fig. S1 of the supplementary material, shows that carbon content decrease with increasing temperature. With regards to the HTL-AP, the TOC, TN, and COD values are shown in Fig. 4.

COD ranged between 44.9 and 56.1 g_{O_2}/L, with the highest COD content detected at 300 °C-10min and 325 °C-10min cases. These values are more than 100-fold higher than the maximum value for European legislation (0.125 g_{O_2}/L), highlighting the need for appropriate treatment and, ideally, valorization.

TOC ranged similarly between 15.2 and 21.6 g_C/L, with the highest value at 300 °C-10min case.

The COD and TC results aligns with the literature data. It should be noted that, despite being similar, COD and TC provide different information. The former refers to degradability, while the latter to the quantitative carbon amount: in the current context, COD is more relevant, as it is the basis for further considerations. High COD levels can lead to higher heat production during WO, favoring the integration between the two technologies, but as the data shows, the highest COD levels coincide with lower biocrude yields.

TN ranges between 737 and 888 mg_N/L, with the highest value observed in the 350 °C-30min case. The ammonia concentration was set to 370 mg/L for each condition based on the average of the available tests.

Literature data on the HTL-AP composition from the co-processing of these two biomass types are currently lacking. Nevertheless, the values obtained in this study are in line with the characteristic ranges reported for the individual processing of manure and lignocellulosic biomass. Specifically, COD, TOC and TN concentrations of approximately 80 g/L, 25 g/L and 10 g/L for manure, and 20 g/L, 14 g/L and 3 g/L for lignocellulosic biomass, have been well-documented (Watson et al., 2020).

The results of the VFA analysis are presented in Table S5 of the supplementary material. Acetic acid was identified as the predominant component, with an average concentration of 6 g/L, followed by propanoic acid at 1 g/L. Other volatile fatty acids were detected in trace amounts.

Table 1
Specific consumption and outlet pressure for different oxygen production technologies.

	P_{prod} (bar)	$SC\left(\frac{kWh}{Nm^3_{O_2}}\right)$	Ref.
Electrolyzer (PEM)	30	1.48	(H-TEC SYSTEMS)
Pressure swing adsorption (PSA)	6	1	(GENERON)
Oxygen transport membrane (OTM)	5	0.2	(Bai et al., 2021; Kriegel, 2014)

3.2. Optimal HTL-WO process configuration

Fig. 5 shows the optimal process scheme configuration revealed by the pinch point analysis. It employs four countercurrent heat exchangers and two trim heaters, in case of non-autothermal scenario. Specifically, the first trim heater (TH1) (between stream 5–6, before the HTL reactor) is used to heat up the inlet of HTL (stream 5) to temperature setpoint when $T_{setHTL} = 350$ °C. The second trim heater (TH2) is required when the inlet temperature of wet oxidation (stream 16) cannot be reached with the heat exchanger" HEX WO-WO''. It must be remembered that for the analysis a delta T minimum of 15 °C was used.

The identified network offers several advantages. First, the network avoids the need for fluid splitting, which could present challenges in practical implementation.

Additionally, it is highly flexible, allowing efficient management of the involved streams, ensuring that even with variations in process mass yields, the system maintains thermal integration. The HTL-WO integration could achieve an autothermal configuration in some conditions with just two heat exchangers by combining the WO output with the HTL input; however, this approach could lead to issues related to mismatched mass flow rates between the two streams. Instead for the proposed scheme the reliability in thermal integration is achieved by working with the same in-out streams in the heat exchangers that cover

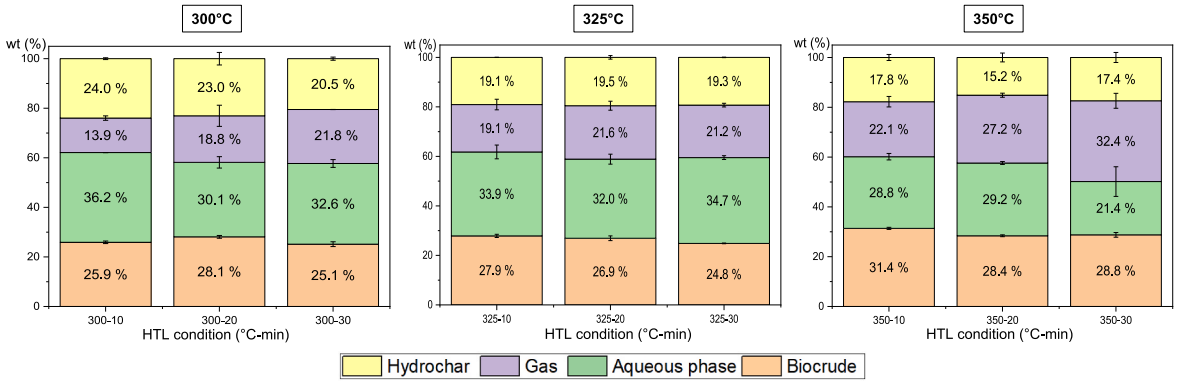

Fig. 3. – Mass yields of the HTL products under different temperatures and residence times.

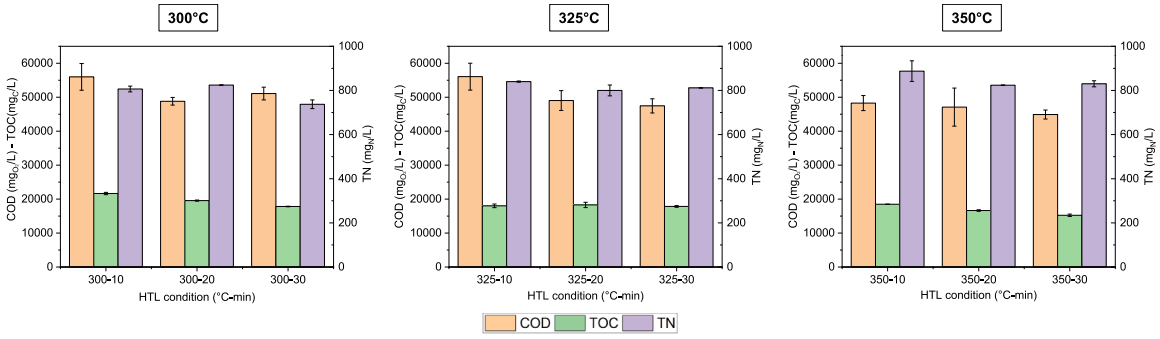

Fig. 4. – COD/TOC and TN analysis results of HTL-AP under different temperatures and residence times.

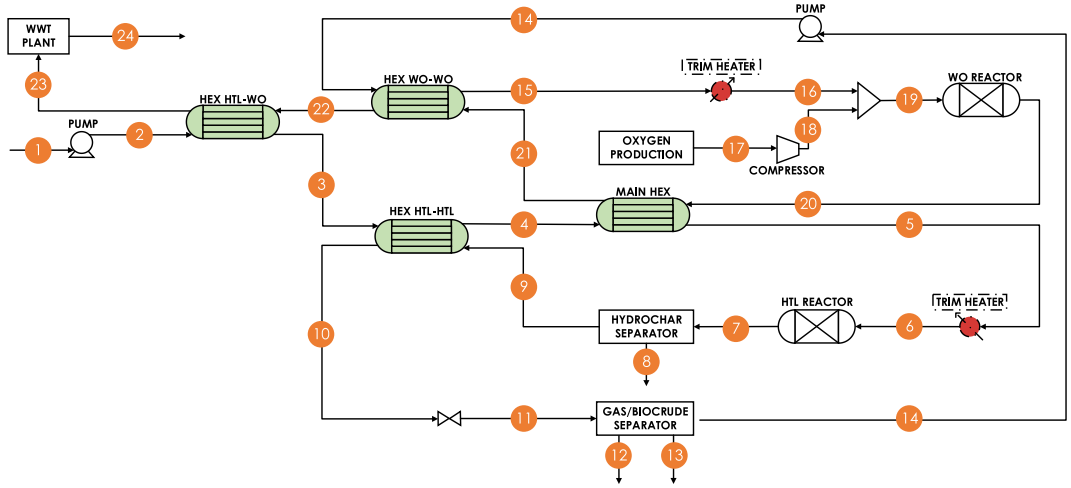

Fig. 5. – Process scheme network for HTL-WO integration. In red the external heat requirement, in green the internal heat recoveries. (For interpretation of the references to colour in this figure legend, the reader is referred to the Web version of this article.)

the largest temperature gradients (HEX HTL-HTL, HEX WO-WO), while those handling streams with different mass flow rates cover smaller temperature ranges (MAIN HEX, HEX HTL-WO). These considerations focus on thermal efficiency, techno-economic evaluation should be added to decide the best configuration including also cost evaluation. Further details are provided in the supplementary material listing the equivalent temperature, pressure, and mass flow rate for each of the numbered streams in Table S4.

After the HTL-WO system, WWT plant is considered, as in the standalone HTL configuration, to reduce the COD level in compliance with European regulations.

3.3. *Wet oxidation process simulations*

The first WO simulations focused just on HTL-AP produced at 325 °C for 20 min to understand process behavior. According to the COD, TC, TN, NH_4, and the VFA analysis, it was possible to make a bulk allocation of the HTL-AP in main compound classes according to the 13 chemical compounds for which kinetic data for WO was available (Schuck et al., 2023). Experimental VFA analysis is reported in Table S5, while the HTL-AP model compound distribution used for the simulation is shown in Table S15.

Oxygen mass flow rate was the first variable analyzed. Fig. 6-A depicts the WO outlet temperature as a function of the oxygen amount

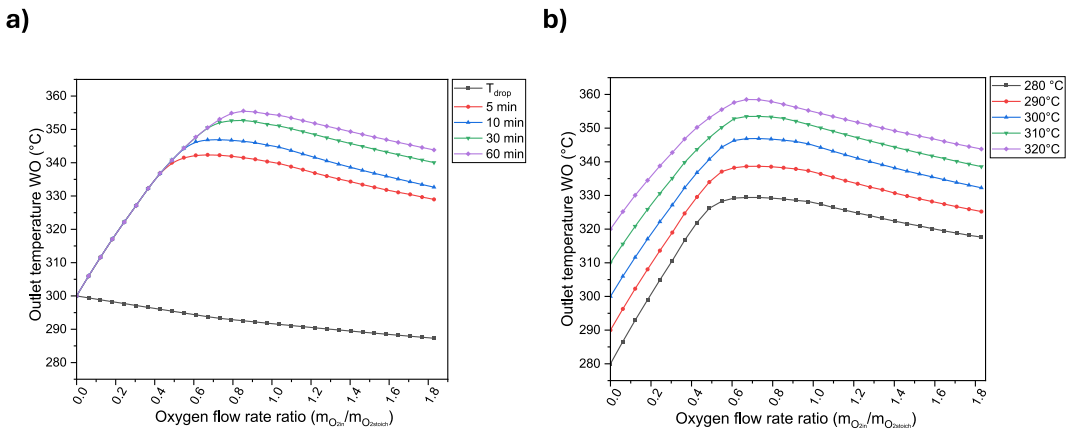

Fig. 6. – Influence of oxygen mass flow rate inlet (expressed as flowrate ratio, with respect to the stoichiometric value) on outlet WO process temperature with 325 °C-20 min HTL-AP varying: a) residence time at constant inlet temperature of 300 °C, b) HTL-AP inlet temperatures at constant residence time of 10 min.

Table 2
Comparison of optimal and stoichiometric oxygen mass flow rates for different reaction time with 325 °C-20min HTL-AP.

	T_{inWO} (°C)	$COD_{removal}$ (%)	$\frac{\dot{m}_{O_{2opt}}}{\dot{m}_{O_{2stoic}}}$ (%)	$O_{2conversion}$ (%)	Reactor length (m)[a]
5 min stoic.	316	55 %	55 %	62 %	340
5 min opt.	311	49 %		97 %	287
10 min stoic.	309	61 %	61 %	68 %	667
10 min opt.	305	55 %		99 %	557
30 min stoic.	298	71 %	73 %	78 %	1955
30 min opt.	296	66 %		97 %	1768
60 min stoic.	290	77 %	82 %	84 %	3827
60 min opt.	289	73 %		96 %	3583

[a] The internal and external diameters of the WO tubes were selected as 49.1 mm and 63 mm, respectively, to ensure pressure resistance and according to availability in the market.

injected in the preheated HTL-AP stream at 300 °C. Regardless of reaction time, increasing the O_2 mass flow rate resulted in an initial rise in the outlet WO temperature due to the exothermic nature of the reaction. However, this increase levelled off, reaching a maximum at a sub-stoichiometric O_2 ratio of 0.65–0.85 (relative to COD). This flow rate can be considered optimal, as it achieves the maximum temperature favorable for reaction kinetics and facilitates further integration of process streams for energy recovery.

The non-monotonous trend in the WO outlet temperature is attributed to a temperature drop (T_{drop}, black line in Fig. 6-a) following the mixing of water and oxygen. This occurs due to the presence of a gas phase (i.e., not dissolved oxygen), leading to evaporation of water (according to Raoult's law), which in turn absorbs heat during the phase change (Sladkovskiy et al., 2018). Further analysis is necessary to define and describe the phenomenon entirely. Operating at over-stoichiometric conditions presents another drawback: incomplete oxygen conversion. As a result, additional energy may be required for separation and recycling processes.

Additionally, this phenomenon prevents the autothermal process from being carried out with air instead of pure oxygen. According to Debellefontaine et al. (1999), the nitrogen portion in air can affect the WO process. As an inert component, nitrogen increases the overall gas flow, which enhances the rate of vaporization. This accelerated vaporization absorbs thermal energy from the system, ultimately lowering the adiabatic reactor temperature.

The optimal oxygen amount increases monotonically with the reaction time. This is because a higher extent of reaction can be expected by increasing the residence time, and hence a higher amount of heat is released that counteracts the temperature drop resulting from using higher O_2 concentrations.

The influence of the WO inlet temperature, in the range between 280 and 320 °C, on the maximum outlet WO temperature at 10 min residence time is reported in Fig. 6-b. It is interesting to note that the maximum is always present in the 0.6–0.8 stoichiometric ratio region. Since the maximum is not dependent on the WO inlet temperature, a constant optimal oxygen amount (0.65) can be used for HTL-WO integration for each HTL conditions in the final comparison with HTL alone.

Following this initial analysis, for the sake of process integration, the maximum WO outlet temperature is set to 350 °C, while the WO inlet temperature is set as a variable of interest.

In Table 2 the WO inlet temperatures required to reach 350 °C are reported for different reaction times showing stoichiometric and optimal oxygen flowrate. These simulations confirm that the amount of oxygen can be optimized by lowering it compared to the stoichiometric amount to reduce T_{inWO} and achieve an outlet temperature of 350 °C. This increases the probability of reaching autothermicity, as less energy is required to reach the WO process inlet temperature. If maximizing water purification is the primary goal, different oxygen flow rates should be considered. As noted earlier, the optimal amount of oxygen increases with reaction time because higher conversions are reached, and more heat is released. COD removal is higher with stoichiometric oxygen amounts, as can be expected, due to its increased concentration, which facilitates more oxidation reactions.

As noted earlier, another advantage of working at optimal oxygen amount is represented by its conversion, which has to be minimized as much as possible, as oxygen represents a valuable product that requires significant energy for production. For example, at 5 min, the oxygen conversion is 62 % at the stochiometric conditions, while it is 97 % at the

optimal ones. This is reflected in the WO gaseous outlet where oxygen presence is almost negligible (Table S6 in Supplementary material).

As expected, COD removal increases with reaction time, as confirmed by previous studies (Schuck et al., 2023; Silva Thomsen et al., 2022, 2024). Compared to the results of Silva Thomsen et al. (2022) the removals are lower. This is because the previous study was conducted in isothermal mode, whereas these simulations consider an adiabatic reactor. Moreover, the HTL feedstock differs, as sewage sludge HTL-AP was used in the referenced work, resulting in significantly varied water compositions.

Despite longer reaction times (30 and 60 min) achieve COD removals exceeding 70 %, the required reactor lengths (1.77–3.83 km) render these conditions unsuitable for practical application. For the following part of the work, a 700 m reactor was employed. This specific length was selected to provide realistic dimensions and good COD removals for comparative purposes for the different HTL-AP conditions. The reactor is designed to be made of 58 U-shaped tubes, each with a length of 12 m, running back and forth.

Based on the considerations on the optimal quantities of oxygen, it was decided to model an injected amount equal to 65 % of the stoichiometric quantity. The involved flow rates, according to the experimental results reported in paragraph 3.1, ranged between 0.868 and 0.886 kg/s for HTL-AP (considering the humidity retained by the hydrochar) and between 0.027 and 0.034 kg/s for the corresponding oxygen. With these mass flow rates an average residence time of ca. 12 min was determined. Hence this condition was evaluated, for each HTL-AP case, to identify the inlet temperature that resulted in the WO outlet temperature of 350 °C.

As depicted in Fig. 7, for different COD concentrations and consequently different injected oxygen amounts, different temperatures are required at the WO reactor inlet to reach 350 °C. Higher COD concentrations result in a lower inlet temperature requirement in the WO reactor to reach 350 °C, as more heat is generated by the oxidation reactions. Therefore, lower time and temperature HTL conditions may favor an autothermal process due to the COD content enabling a greater temperature gradient in the WO reactor. Nevertheless, it is important to note that these conditions can adversely affect both the yield and quality of the biocrude.

The COD removals were on average 57.6 % ± 0.4 %. It exhibits almost constant values across the different cases, mainly because the different HTL-AP compositions are modeled with comparable percentages of the same compounds (see Table S15). Given that the resulting water contains a COD higher than 20 g/L after the WO process, additional treatment is necessary (as reported in section 3.2 of process configuration). Moreover, a comprehensive experimental evaluation of the pollutants is essential for the technology's further development.

Liquid and gaseous phases outlet compositions after the flash separation are reported in Table S6 and Table S7. The WO outlet gaseous stream is mainly composed of CO_2, with an average molar composition of 89 %. The remaining composition follows a descending order of oxygen, nitrogen, and water. This high CO_2 concentration can make the outlet gas suitable for CCUS applications, as higher CO_2 concentrations in the waste stream make the capture process more efficient and cost-effective (IEA, 2019). Oxygen conversion was monitored across all HTL-AP conditions, revealing minimal wastage with conversion rates between 95 % and 97 %.

The remaining COD content in WO processed water consists primarily of acetic acid, accounting for 67.0 %–70.5 % of the residual COD. This is due to acetic acid being an intermediate product of other compounds oxidation and being resistant to oxidation, higher temperatures are needed for his conversion (Debellefontaine et al., 1999; Silva Thomsen et al., 2022). Understanding this concentration is crucial for the potential utilization of acetic acid as a byproduct.

3.4. HTL-WO integration and HTL standalone power requirements

Overall power requirements for different HTL conditions were considered and compared in the configurations of standalone HTL and HTL-WO integration. Heat duties are reported in Table 3.

In the HTL standalone configuration, the trim heaters power requirement by the HTL slurry heating is always substantial. The heat requirement for TH1 is constant in HTL condition because the same slurry inlet must face the temperature step from the ambient temperature before entering in HEX HTL-HTL. On the other hand, TH2 has to heat up the slurry to the HTL set temperature after the HEX HTL-HTL, which has a different outlet temperature according to the condition.

Concerning the HTL-WO integration configuration, the results are very encouraging, demonstrating the possibility of autothermal operation, in several conditions when HTL set temperature is 300 and 325 °C.

In contrast, for all cases involving HTL at 350 °C, a constant amount of heat from TH2 is required. This heat is necessary to raise the slurry temperature from 335 °C to 350 °C, ensuring the pinch point ΔT_{min} of 15 °C. Consequently, in the 350 °C HTL case, the heat duty of HEX MAIN decreases significantly because the trim heater compensates for most of the heat required to reach the HTL set temperature. From a theoretical perspective, achieving autothermal operation at 350 °C HTL conditions

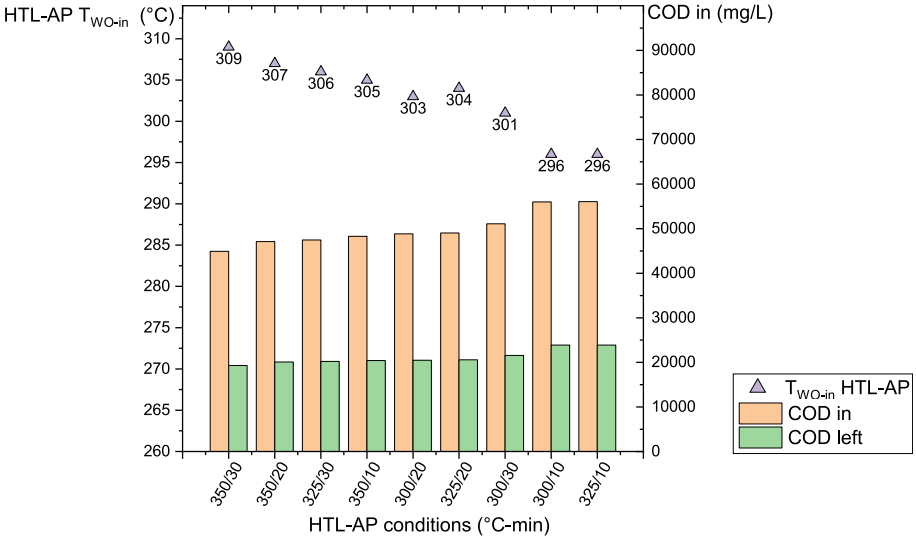

Fig. 7. Inlet temperature of each HTL-AP condition to exit from WO process at 350 °C comparison with COD (modeled outlet COD error bars are derived from inlet experimental standard deviations).

Table 3
Heat exchanger and trim heaters thermal load (kW) in HTL standalone and HTL-WO integration layout for different HTL conditions (°C-min).

HTL standalone									
	300–10	300–20	300–30	325–10	325–20	325–30	350–10	350–20	350–30
HEX HTL-HTL	965.5	967.7	973.7	1109.8	1108.5	1109.2	1271.2	1278.8	1272.4
TH heat losses HTL	2.5	3.2	3.6	2.8	3.5	4.0	3.2	4.0	4.5
TH 1	152.1	152.1	152.1	152.1	152.1	152.1	152.1	152.1	152.1
TH 2	128.4	125.7	118.8	121.3	122.9	122.5	127.3	123.1	126.3
THTotal	235.7	236.4	236.8	244.5	245.2	245.7	263.8	264.6	265.2
HTL-WO integration									
	300–10	**300–20**	**300–30**	**325–10**	**325–20**	**325–30**	**350–10**	**350–20**	**350–30**
HEX HTL-HTL	965.5	967.7	973.7	1109.8	1108.5	1109.2	1271.2	1278.8	1272.4
HEX WO-WO	886.0	909.8	906.4	886.5	920.4	934.3	921.6	934.0	929.1
HEX MAIN	121.7	119.2	112.8	115.1	116.7	116.3	18.2	14.4	17.4
HEX HTL-WO	144.9	144.9	146.2	144.6	145.6	143.7	145.7	144.7	146.4
TH heat losses HTL	2.5	3.2	3.6	2.8	3.5	4.0	3.2	4.0	4.5
TH 1	0.0	0.0	0.0	0.0	0.0	0.0	108.6	108.6	108.6
TH 2	0.0	0.0	0.0	0.0	0.0	0.0	0.0	0.0	0.0
TH_{Total}	2.5	3.2	3.6	2.8	3.5	4.0	111.8	112.5	113.1

is possible if the WO process operate at higher temperatures, at least 365 °C, hence maintaining a ΔT_{min} of 15 °C.

Regarding the pump electrical expenditures (Table S8 and Table S9), in both the HTL-WO and HTL standalone configurations, to pump the slurry requires 36.7 kW. In the HTL-WO integration configuration, the power requirements to pump the aqueous phase varies slightly, ranging between 22.2 and 22.6 kW, depending on the AP and hydrochar yield. The energy consumption of pumping slurry is significantly higher than the HTL-AP due to differences in fluid characteristics. Specifically, a lower efficiency of 0.6 was considered to pressurize the slurry, compared to 0.9 for the HTL-AP.

In the HTL-WO integrated process, the power requirements for oxygen production (Table S10) and compression are crucial factors. Compression energy depends significantly on the outlet pressure of each technology. As noted in paragraph 2.3.3, electrolyzers generate oxygen at higher pressures than PSA systems and membranes, reducing the compression ratio needed to reach the target of 220 bar. Specifically, oxygen compression requires between 5.5 and 7.1 kW for electrolyzers, 10.8 and 13.8 kW for PSA systems, 11.5 and 14.6 kW for membranes. However, the power consumption for oxygen production is more significant: electrolyzers require between 99.4 and 126.6 kW, PSA systems between 62.0 and 79.0 kW, while membrane technology only 12.4–15.8 kW. Overall, the innovative, not yet commercial, membrane technology results as the least energy-intensive option, with energy costs averaging 4.4 times lower than electrolyzers and 3 times lower than PSA systems.

The last power expenditure is represented by the wastewater treatment plant. Before disposal, the HTL-AP must be cleaned to reduce its COD to reach EU discharge limits. This applies to both configurations, which results between 125.9 and 160.5 kW for HTL stand-alone and between 53.2 and 67.8 kW for HTL-WO integration (Table S11 and Table S12). The use of WO significantly reduces the power expenditure of the wastewater treatment plant. The percentage reduction between the two configurations is directly proportional to the COD removed by the WO process. 2.3.3.

The power expenditures distributions for the HTL standalone configuration and HTL-WO integration with various oxygen production technologies are illustrated in Fig. 8. HTL standalone case at 325 °C and 20 min is compared with the HTL-WO integration in the same condition where, autothermicity is reached. Moreover, the power expenditures are also reported for the not autothermal HTL-WO integration at 350 °C-20 min.

In the HTL standalone configuration, heating represents the largest portion of power consumption, accounting for 61 % of the total demand. This is followed by the energy required for the WWT plant and the pump, which contributed 31 % and 8 %, respectively. The total power demand for this configuration amounts to 455.0 kW.

In the HTL-WO integration at 325 °C-20 min, where autothermal conditions are achieved, there is a notable decrease in the trim heater's heat duty, leading to a minimal contribution of around 2 % to the total power expenditure.

Oxygen production and compression become significant factors in the power demand, with their impact varying based on the technology used. When electrolyzers and PSA systems are utilized, oxygen production is relevant, accounting for 19 %–49 % of the total expenditure. In contrast, membrane technology is less significant.

The power demand for pumping is higher compared to the HTL standalone configuration due to the addition of a second pumping stage to pressurize the HTL-AP for the WO, resulting in pump-related expenditures ranging from 25 % to 39 % of the total power demand.

Overall, the total power expenditure for the HTL-WO integration, when autothermicity is achieved drops between 150.5 kW and 238.8 kW, depending on the oxygen production technology, representing a reduction of 42 %–64 % compared to the HTL standalone configuration.

The final scenario considered is the HTL-WO integration at 350 °C-20 min, where autothermal conditions are not met. In this case, heating demands constitute a moderate portion of the power expenditures, though they remain lower than in the HTL standalone configuration. The total power demand in this configuration ranges from 256.0 kW to 340.7 kW, still achieving a reduction of 25 %–44 % compared to the HTL standalone configuration in the same condition (at 350 °C/20min), not reported in figure.

To assess the energetic viability of the process schemes, it is crucial to evaluate the final power output contained in the biocrude, which remains consistent across both process configurations. The results, presented in Table 4, indicate that the biocrude's energy content remains relatively stable for the 300 °C and 325 °C cases. However, it increases at 350 °C due to a higher heating value (HHV) resulting from an elevated carbon content.

3.5. Energy return on investment evaluation

The energy return on investment (EROI) was identified as a useful metric for comparing the benefits of HTL-WO integration versus the HTL standalone process. A higher EROI indicates a more sustainable process, as it reflects greater energy output relative to the energy consumed. For hydrothermal processing, the EROI typically falls between 1 and 3, making it competitive with traditional biofuels production technologies (Adams et al., 2017).

Starting from the standalone configuration, as depicted in Fig. 9, EROI ranges between 2.3 and 3.0. These values fall at the upper

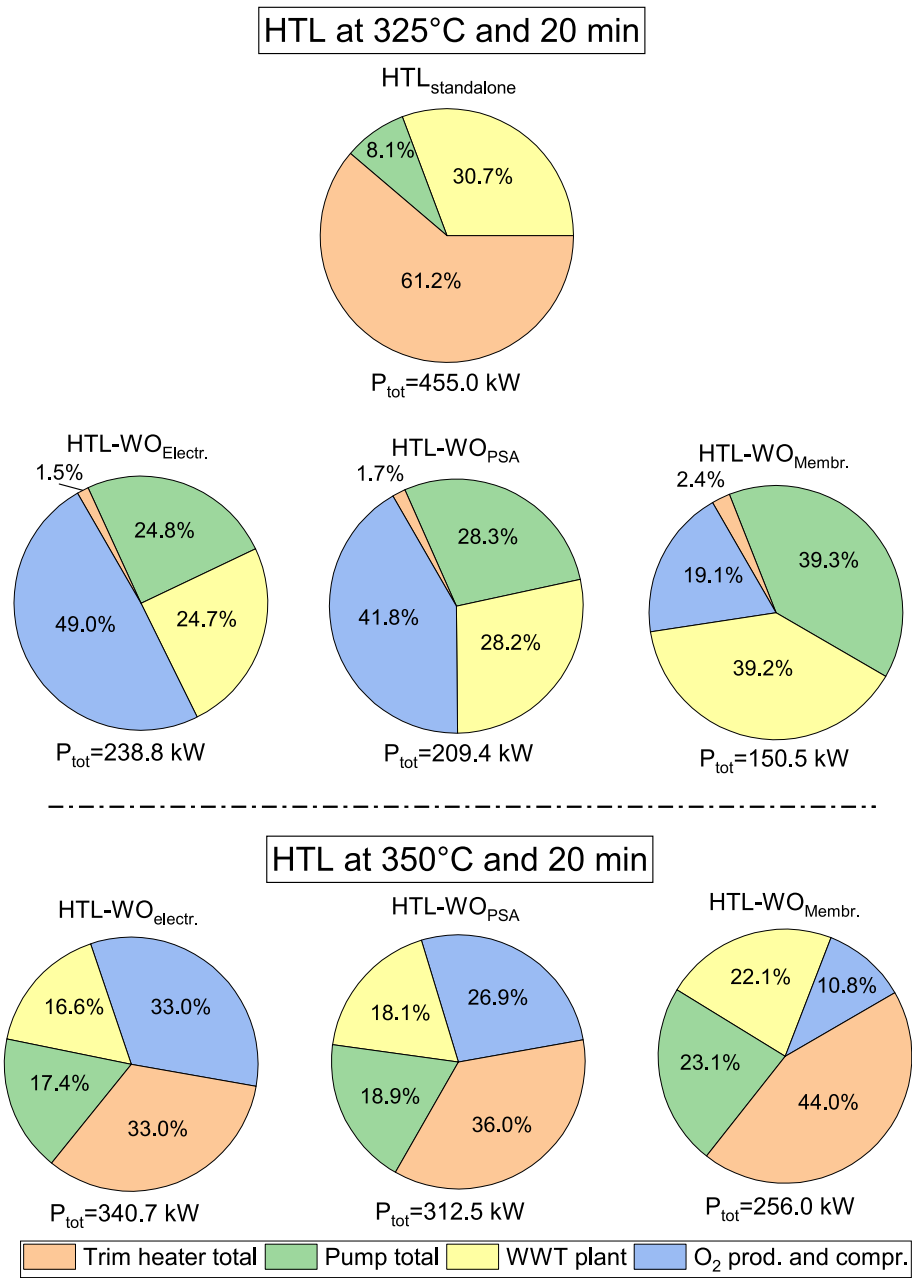

Fig. 8. – Total power requirements and distribution representation for three process conditions with different oxygen production technology.

Table 4
HTL biocrude power content for the different conditions.

HTL cond. (°C-min)	300–10	300–20	300–30	325–10	325–20	325–30	350–10	350–20	350–30
$P_{biocrude}$ (kW)	1113.5	1239.6	1127.8	1136.7	1172.2	1171.6	1350.9	1363.1	1347.7

boundary of the previously mentioned range due to the absence of energy input required for the feedstock harvesting, which consists of agricultural waste.

Considering previous studies on the EROI of agricultural waste, average EROI of approximately 2 are reported (Cheng et al., 2020), accounting for wider system boundaries, including biocrude upgrading. When excluding this factor, the results presented in this study are consistent with those reported in the literature. To compare with studies having similar system boundaries, the EROI in this study are slightly lower than the previously estimated values of 5.5 and 4.3 for HTL of sewage sludge (Hussain and Anastasakis, 2025; Maqbool et al., 2024). This is mainly due to the lower biocrude yields and HHVs in the present study (24.8–31.4 wt % and 27.1–32 MJ/kg, respectively) compared to the cited articles (29.2–32.2 wt % and 33.6–35.8 MJ/kg, respectively) as well as to the lower DM content of the slurry utilized herein (15 wt % vs 20 wt %).

In this study the highest EROI values are observed at elevated temperatures, attributed to increased energy outputs resulting from higher HHV and reduced power requirements for WWT due to lower organic content in the water.

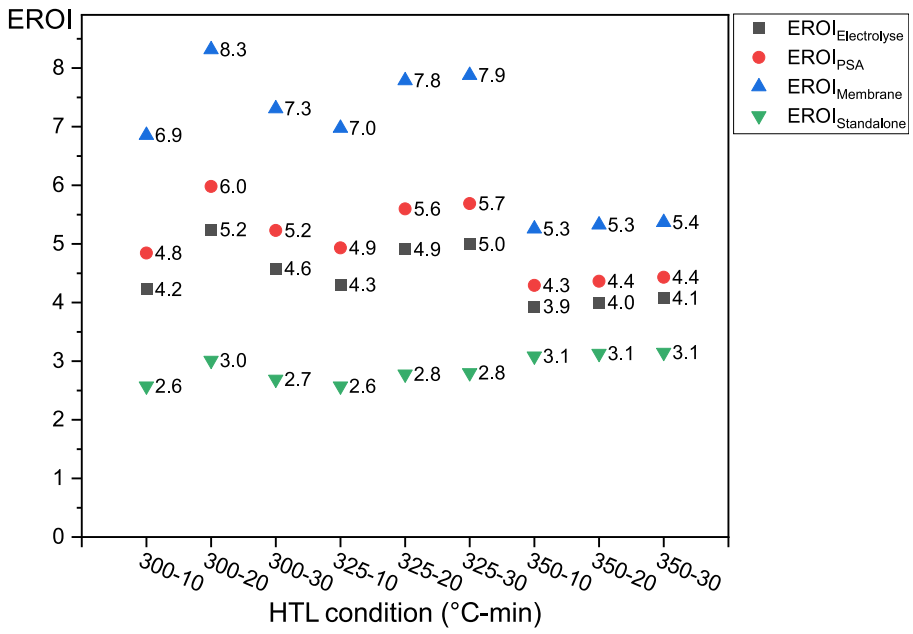

Fig. 9. EROI of HTL standalone process and HTL-WO integration at different conditions.

Shifting towards the HTL-WO integration it becomes evident that incorporating WO significantly enhances process efficiency. According to the different scenarios, WO integration can increase the EROI between 1.3 and 3.0 fold with respect to the HTL standalone configuration. This variation mainly depends on which oxygen production technology is used.

The highest EROI value, reaching 8.3, was observed under the HTL condition of 300 °C for 20 min, coupled with WO and utilizing membrane transport for oxygen production technology. However, it is important to remember that this technology is currently at low TRL. Given the current state of the art, the best-case scenario likely would involve PSA, which achieves EROI of 6.0. This HTL condition (300 °C-20 min) proved to be the most effective due to the achievement of autothermal operation and a good balance of biocrude yield and HHV.

It is important to note that, even though autothermal operation are not achieved at 350 °C in the HTL process, the EROI increases with respect to standalone configuration. This is because the higher energy expenditures are offset by the increased energy content of the biocrude produced at this temperature. This finding highlights how the benefits of HTL-WO integration are robust with respect to the HTL reaction temperature and time.

An optimal operating point for the HTL-WO process could be found by balancing temperature and reaction time of both HTL and WO. Ideally, this would involve conditions where COD is reduced for WWT and external heat expenditures are minimized.

To compare HTL-WO integration with other AP treatment strategies EROI results were extracted from techno-economic analyses. Specifically Tito et al., 2023 investigated aqueous phase reforming for hydrogen production, achieving a maximum EROI of 2.4, with differences in the system boundaries (the upgrading step is included), assumptions (e.g. hydrochar is burned as thermal source) and feedstock (corn stover and lignin-residue). Additionally, aqueous phase treatment via partial oxidation integrating Fischer-Tropsch synthesis and the aqueous phase recirculation, reported EROIs respectively of 1.7 and 2.1 (Hansen et al., 2019; Pedersen et al., 2018). Anaerobic digestion, have shown promising results as treatment for the HTL-AP with 84.5 % of energy recovery (bio-crude and biomethane) from biomass, reducing COD of HTL-AP by 48–57 % (Kaur Tatla et al., 2024; Zoppi et al., 2023). The integration of HTL with anaerobic digestion (HTL-AD) resulted in an equivalent EROI of up to 3.2 (Adedeji et al., 2024). These comparisons show that the integration of HTL with WO can more than double the energy return compared to other treatment strategies for the aqueous phase.

EROI values for the HTL-WO integration are highly promising also when compared to those of other biofuel technologies (lower than 4). These values are surpassed only by sugar beet ethanol (EROI = 11.26); however, sugar beet ethanol is not classified as an advanced biofuel and competes with food production (Prananta and Kubiszewski, 2021; Wang et al., 2021).

WO integration has the potential to enhance the environmental sustainability of HTL, aligning with the principles of green chemistry. In particular, the valorization of the wastewater stream adheres to the first principle of green chemistry, as formulated by Paul Anastas, by minimizing waste generation in chemical processes (Anastas and Eghbali, 2010). Additionally, heat integration supports the sixth principle, which advocates for reducing external energy inputs. Overall, the approach proposed in this study has the potential to lower fossil CO_2 emissions; however, a more thorough evaluation using a life-cycle-assessment is required to quantify its impact.

4. Conclusion

The co-production of a contaminated aqueous stream and the high energy demand are two of the key challenges in the development of hydrothermal liquefaction. In this work, deployment of wet oxidation is presented as a promising process to address both challenges simultaneously.

Two process configurations were studied: one for standalone HTL and one for the HTL-WO integration. The study revealed that wet oxidation can make the overall process autothermal. The HTL-WO integration achieved a notable reduction in overall energy consumption, ranging from 25 to 67 % compared to HTL alone. This results in a robust process that remains resilient to variations in HTL operative parameter, making this combined approach a promising option for scaling HTL technology industrially for biofuel production.

These findings are supported by the evaluation of the EROI, which increased by 1.3–3.0 fold with HTL-WO integration compared to the standalone HTL configuration. The most significant variable influencing HTL-WO efficiency improvements is the technology of oxygen production for the WO process.

In conclusion, further investigation into the WO process through targeted simulations and experimental studies is essential to refine its operational parameters and integration potential. Additionally, comprehensive techno-economic and life cycle assessments will be required to fully evaluate the overall sustainability of the HTL-WO system. Given that much of the foundational data has already been gathered in this study, these analyses would serve as a valuable follow-up to guide future developments and scalability.

CRediT authorship contribution statement

Guido Ceragioli: Formal analysis, Writing – original draft, Investigation, Writing – review & editing, Methodology, Data curation, Conceptualization. **Carolin Eva Schuck:** Validation, Writing – review & editing, Methodology. **Giulia Zoppi:** Investigation, Data curation, Validation, Methodology, Formal analysis, Writing – review & editing, Supervision. **Giuseppe Pipitone:** Validation, Data curation, Writing – review & editing, Supervision. **Konstantinos Anastasakis:** Validation, Methodology, Writing – review & editing, Supervision, Formal analysis. **Samir Bensaid:** Supervision, Writing – review & editing. **Raffaele Pirone:** Supervision, Writing – review & editing. **Patrick Biller:** Writing – review & editing, Supervision, Funding acquisition, Conceptualization, Validation, Resources, Data curation.

Declaration of competing interest

The authors declare the following financial interests/personal relationships which may be considered as potential competing interests: Patrick Biller reports financial support was provided by European Union. If there are other authors, they declare that they have no known competing financial interests or personal relationships that could have appeared to influence the work reported in this paper.

Acknowledgement

Funded by the European Union under GA No. 101083944 (project CIRCULAIR). Views and opinions expressed are however those of the author(s) only and do not necessarily reflect those of the European Union or CINEA. Neither the European Union nor the granting authority can be held responsible for them.

We thank Francesca Stella for her help in creating the graphical abstract.

Appendix A. Supplementary data

Supplementary data to this article can be found online at https://doi.org/10.1016/j.jclepro.2025.146242.

Data availability

Data will be made available on request.

References

Adams, P., Bridgwater, T., Lea-Langton, A., Ross, A., Watson, I., 2017. Biomass conversion technologies. In: Greenhouse Gas Balances of Bioenergy Systems. Elsevier, pp. 107–139. https://doi.org/10.1016/B978-0-08-101036-5.00008-2.

Adedeji, O.M., Aboagye, E.A., Oladoye, P.O., Bauer, S.K., Jahan, K., 2024. Life cycle assessment and net energy analysis of an integrated hydrothermal liquefaction-anaerobic digestion of single and mixed beverage waste and sewage sludge. Chemosphere 363. https://doi.org/10.1016/j.chemosphere.2024.142991.

Anastas, P., Eghbali, N., 2010. Green chemistry: principles and practice. Chem. Soc. Rev. 39, 301–312. https://doi.org/10.1039/b918763b.

Anastasakis, K., Biller, P., Madsen, R.B., Glasius, M., Johannsen, I., 2018. Continuous hydrothermal liquefaction of biomass in a novel pilot plant with heat recovery and hydraulic oscillation. Energies (Basel) 11. https://doi.org/10.3390/en11102695.

Bai, W., Feng, J., Luo, C., Zhang, P., Wang, H., Yang, Y., Zhao, Y., Fan, H., 2021. A comprehensive review on oxygen transport membranes: development history, current status, and future directions. Int. J. Hydrogen Energy. https://doi.org/10.1016/j.ijhydene.2021.08.177.

Biller, P., Madsen, R.B., Klemmer, M., Becker, J., Iversen, B.B., Glasius, M., 2016. Effect of hydrothermal liquefaction aqueous phase recycling on bio-crude yields and composition. Bioresour. Technol. 220, 190–199. https://doi.org/10.1016/j.biortech.2016.08.053.

Channiwala, S.A., Parikh, P.P., 2002. A unified correlation for estimating HHV of solid, liquid and gaseous fuels. Fuel 81. https://doi.org/10.1016/S0016-2361(01)00131-4.

Cheng, F., Porter, M.D., Colosi, L.M., 2020. Is hydrothermal treatment coupled with carbon capture and storage an energy-producing negative emissions technology? Energy Convers. Manag. 203. https://doi.org/10.1016/j.enconman.2019.112252.

Council of the European Union, 1991. Council directive of 21 May 1991. https://eur-lex.europa.eu/eli/dir/1991/271/oj/eng. (Accessed 1 November 2024).

Debellefontaine, H., Foussard, J.N., 1999. Wet air oxidation for the treatment of industrial wastes. Chemical aspects, reactor design and industrial applications in Europe. Waste Manag.

Debellefontaine, H., Crispel, S., Reilhac, P., Périé, F., Foussard, J.N., 1999. Wet air oxidation (WAO) for the treatment of industrial wastewater and domestic sludge. Design of bubble column reactors. Chem. Eng. Sci. 54, 4953–4959. https://doi.org/10.1016/S0009-2509(99)00217-1.

Dietrich, M.J., Randall, T.L., Canney, P.J., 1985. Wet air oxidation of hazardous organics in wastewater. Environ. Prog. 4. https://doi.org/10.1002/ep.670040312.

Dos Passos, J.S., Matayeva, A., Biller, P., 2022. Synergies during hydrothermal liquefaction of cow manure and wheat straw. J. Environ. Chem. Eng. 10. https://doi.org/10.1016/j.jece.2022.108181.

GENERON, 2024. PSA oxygen generator. https://www.generon.com/product/psa-oxygen-generator/. (Accessed 1 November 2024).

Ghadge, R., Nagwani, N., Saxena, N., Dasgupta, S., Sapre, A., 2022. Design and scale-up challenges in hydrothermal liquefaction process for biocrude production and its upgradation. Energy Convers. Manag. X. https://doi.org/10.1016/j.ecmx.2022.100223.

H-TEC SYSTEMS, 2024. PEM electrolyzer ME450. https://www.hannovermesse.de/apollo/hannover_messe_2024/obs/Binary/A1333922/H-TEC-Datenblatt-ME450-EN-24-03.pdf. (Accessed 1 November 2024).

Hansen, N.H., Pedersen, T.H., Rosendahl, L.A., 2019. Techno-economic analysis of a novel hydrothermal liquefaction implementation with electrofuels for high carbon efficiency. Biofuel Bioprod. Biorefining 13, 660–672. https://doi.org/10.1002/bbb.1977.

He, S., Wang, J., Cheng, Z., Dong, H., Yan, B., Chen, G., 2021. Synergetic effect and primary reaction network of corn cob and cattle manure in single and mixed hydrothermal liquefaction. J. Anal. Appl. Pyrolysis 155. https://doi.org/10.1016/j.jaap.2021.105076.

Horschig, T., Penke, C., Habersetzer, A., Batteiger, V., 2020. Regional feedstock potentials and preference regions for HTL projects. Hy Flex Fuel Report, 2020. https://ec.europa.eu/research/participants/documents/downloadPublic?documentIds=080166e5e22545e6&appId=PPGMS.

Hussain, A., Anastasakis, K., 2025. Technoeconomic evaluation of integrating hydrothermal liquefaction in wastewater treatment plants. Bioresour. Technol. 419. https://doi.org/10.1016/j.biortech.2024.132030.

IEA, 2019. The Role of CO2 Storage. IEA, Paris. https://www.iea.org/reports/the-role-of-co2-storage. Licence: CC BY 4.0.

IEA, 2021. Net Zero by 2050. IEA, Paris. https://www.iea.org/reports/net-zero-by-2050, Licence:CCBY4.0.

IEA, 2023. Energy Statistics Data Browser. IEA, Paris. https://www.iea.org/data-and-statistics/data-tools/energy-statistics-data-browser.

ISO. Global standards for trusted goods and services, 2022. ISO 18122:2022: solid biofuels - determination of ash content. https://www.iso.org/standard/83190.html. (Accessed 1 November 2024).

Kaur Tatla, H., Niknejad, P., Ismail, S., Adnan Khan, M., Gupta, R., Ranjan Dhar, B., 2024. A comprehensive assessment of integrating anaerobic digestion and hydrothermal liquefaction processes: harnessing energy from sewage sludge. Energy Convers. Manag. 322. https://doi.org/10.1016/j.enconman.2024.119187.

Kilgore, U.J., Subramaniam, S., Fox, S.P., Cronin, D.J., Guo, M.F., Schmidt, A.J., Ramasamy, K.K., Thorson, M.R., 2023. Wet air oxidation of HTL aqueous waste. Biomass Bioenergy 176, 106889. https://doi.org/10.1016/J.BIOMBIOE.2023.106889.

Kriegel, R., 2014. Fraunhofer IKTS annual report 2013/2014, 76-77. https://www.ikts.fraunhofer.de/content/dam/ikts/downloads/annual_reports/jb2013/Fraunhofer_IKTS_2013_Annual_Report.pdf. (Accessed 1 November 2024).

Kulikova, Y., Klementev, S., Sirotkin, A., Mokrushin, I., Bassyouni, M., Elhenawy, Y., El-Hadek, M.A., Babich, O., 2023. Aqueous phase from hydrothermal liquefaction: composition and toxicity assessment. Water (Switzerland) 15. https://doi.org/10.3390/w15091681.

Lambert, J.G., Hall, C.A.S., Balogh, S., Gupta, A., Arnold, M., 2014. Energy, EROI and quality of life. Energy Policy 64, 153–167. https://doi.org/10.1016/j.enpol.2013.07.001.

Lu, J., Watson, J., Liu, Z., Wu, Y., 2022. Elemental migration and transformation during hydrothermal liquefaction of biomass. J. Hazard. Mater. https://doi.org/10.1016/j.jhazmat.2021.126961.

Madsen, R.B., Christensen, P.S., Houlberg, K., Lappa, E., Mørup, A.J., Klemmer, M., Olsen, E.M., Jensen, M.M., Becker, J., Iversen, B.B., Glasius, M., 2015. Analysis of organic gas phase compounds formed by hydrothermal liquefaction of dried distillers grains with Solubles. Bioresour. Technol. 192, 826–830. https://doi.org/10.1016/J.BIORTECH.2015.05.095.

Maqbool, W., Biller, P., Anastasakis, K., 2024. A kinetic process model for sewage sludge hydrothermal liquefaction in Aspen Plus: model validation with pilot-plant data and

scale up. Energy Convers. Manag. 302. https://doi.org/10.1016/j.enconman.2024.118136.
Matayeva, A., Biller, P., 2021. Hydrothermal liquefaction aqueous phase treatment and hydrogen production using electro-oxidation. Energy Convers. Manag. 244. https://doi.org/10.1016/j.enconman.2021.114462.
Mazhkoo, S., Soltanian, S., Odebiyi, H.O., Norouzi, O., Ubene, M., Hayder, A., Pourali, O., Santos, R.M., Brown, R.C., Dutta, A., 2025. Process intensification in hydrothermal liquefaction of biomass: a review. J. Environ. Chem. Eng. https://doi.org/10.1016/j.jece.2025.115722.
Mishra, N., Reddy, R., Kuila, A., Rani, A., Nawaz, A., Pichiah, S., 2017. A review on advanced oxidation processes for effective water treatment. Curr. World Environ. 12. https://doi.org/10.12944/cwe.12.3.02.
Moser, L., Portner, B.W., Penke, C., Ebner, K., Batteiger, V., 2023. Life-cycle assessment of renewable fuel production via hydrothermal liquefaction of manure in Germany. Sustain. Energy Fuels 7, 4898–4913. https://doi.org/10.1039/d3se00646h.
Pedersen, T.H., Hansen, N.H., Pérez, O.M., Cabezas, D.E.V., Rosendahl, L.A., 2018. Renewable hydrocarbon fuels from hydrothermal liquefaction: a techno-economic analysis. Biofuel Bioprod. Biorefining 12, 213–223. https://doi.org/10.1002/bbb.1831.
Prananta, W., Kubiszewski, I., 2021. Assessment of Indonesia's future renewable energy plan: a meta-analysis of biofuel energy return on investment (eroi). Energies (Basel) 14. https://doi.org/10.3390/en14102803.
Prasad Vadlamudi, D., Gen Lei, X., Goldfarb, J.L., William Tester, J., 2024. Wet oxidation of aqueous phase byproducts from uncatalyzed and acid-catalyzed hydrothermal liquefaction of manure. Chem. Eng. J. 498. https://doi.org/10.1016/j.cej.2024.155524.
Pruden, B.B., Le, H., 1976. Wet air oxidation of soluble components in waste water. Can. J. Chem. Eng. 54, 319–325. https://doi.org/10.1002/cjce.5450540413.
Ramirez, J.A., Brown, R.J., Rainey, T.J., 2015. A review of hydrothermal liquefaction bio-crude properties and prospects for upgrading to transportation fuels. Energies (Basel). https://doi.org/10.3390/en8076765.
Schuck, C.E., Schäfer, T., Anastasakis, K., 2023. Predictive modeling and scale-up of wet oxidation for hydrothermal liquefaction process water treatment. Comput. Aided Chem. Eng. 52, 2229–2234. https://doi.org/10.1016/B978-0-443-15274-0.50355-3.
Shende, R.V., Levee, J., 1999. Wet oxidation kinetics of refractory low molecular mass carboxylic acids. Ind. Eng. Chem. Res. 38, 3830–3837. https://doi.org/10.1021/ie9902028.
Silva Thomsen, L.B., Anastasakis, K., Biller, P., 2022. Wet oxidation of aqueous phase from hydrothermal liquefaction of sewage sludge. Water Res. 209, 117863. https://doi.org/10.1016/J.WATRES.2021.117863.
Silva Thomsen, L.B., Carregosa, J. de C., Wisniewski, A., Anastasakis, K., Biller, P., 2024. Continuous wet air oxidation of aqueous phase from hydrothermal liquefaction of sewage sludge. J. Environ. Chem. Eng. 12, 112672. https://doi.org/10.1016/j.jece.2024.112672.
Sladkovskiy, Dmitry A., Godina, Lidia I., Semikin, Kirill V., Sladkovskaya, Elena V., Smirnova, Daria A., Murzin, Dmitry Yu, 2018. Process design and techno-economical analysis of hydrogen production by aqueous phase reforming of sorbitol. Chem. Eng. Res. Des. 134, 104–116.
Snowden-Swan, L.J., et al., 2022. Wet waste hydrothermal liquefaction and biocrude upgrading to hydrocarbon fuels: 2022 state of technology. https://www.pnnl.gov/main/publications/external/technical_reports/PNNL-33622.pdf.
Tews, I.J., Garcia-Perez, M., 2022. Advanced oxidative techniques for the treatment of aqueous liquid effluents from biomass thermochemical conversion processes: a review. Energy Fuels. https://doi.org/10.1021/acs.energyfuels.1c03048.
Tito, E., Zoppi, G., Pipitone, G., Miliotti, E., Fraia, A. Di, Rizzo, A.M., Pirone, R., Chiaramonti, D., Bensaid, S., 2023. Conceptual design and techno-economic assessment of coupled hydrothermal liquefaction and aqueous phase reforming of lignocellulosic residues. J. Environ. Chem. Eng. 11. https://doi.org/10.1016/j.jece.2022.109076.
Toor, S.S., Rosendahl, L., Nielsen, M.P., Glasius, M., Rudolf, A., Iversen, S.B., 2012. Continuous production of bio-oil by catalytic liquefaction from wet distiller's grain with solubles (WDGS) from bio-ethanol production. Biomass Bioenergy 36, 327–332. https://doi.org/10.1016/J.BIOMBIOE.2011.10.044.
Wan, J., Gu, J., Zhao, Q., Liu, Y., 2016. COD capture: a feasible option towards energy self-sufficient domestic wastewater treatment. Sci. Rep. 6. https://doi.org/10.1038/srep25054.
Wang, C., Zhang, L., Chang, Y., Pang, M., 2021. Energy return on investment (EROI) of biomass conversion systems in China: meta-Analysis focused on system boundary unification. Renew. Sustain. Energy Rev. 137. https://doi.org/10.1016/j.rser.2020.110652.
Watson, J., Wang, T., Si, B., Chen, W.T., Aierzhati, A., Zhang, Y., 2020. Valorization of hydrothermal liquefaction aqueous phase: pathways towards commercial viability. Prog. Energy Combust. Sci. https://doi.org/10.1016/j.pecs.2019.100819.
Williams, P.E.L., Silveston, P.L., Hudgins, R.R., 1975. Oxidation of butyric acid solutions. Can. J. Chem. Eng. https://doi.org/10.1002/cjce.5450530320.
Zoppi, G., Andrade, T.A., Ward, A.J., Ambye-Jensen, M., Biller, P., 2023. Biorefinery integration of a green protein platform for maximum resource utilization. Clean. Circ. Bioeconomy 6. https://doi.org/10.1016/j.clcb.2023.100064.